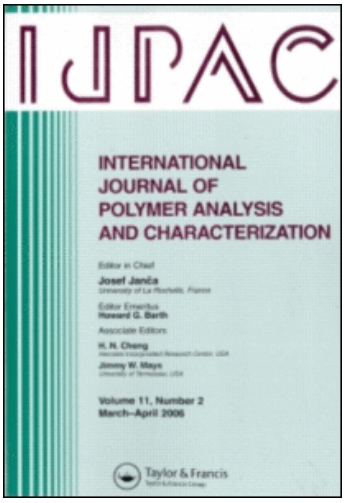

International Journal of Polymer Analysis and Characterization
Publication details, including instructions for authors and subscription information:
http://www.informaworld.com/smpp/title~content=t713646643

Quasi-static Indentation Measurements: A Tool for Micro-mechanical Investigations of Interfaces in Polymer Materials

Bernhard Möginger[a]; Volker Herrmann[b]; Claus Unseld[c]
[a] Fachhochschule Bonn-Rhein-Sieg, University of Applied Sciences, Rheinbach, Germany [b] Degussa Füllstoffsysteme und Pigmente, Köln, Germany [c] Dunlop GmbH, Hanau, Germany

To cite this Article Möginger, Bernhard , Herrmann, Volker and Unseld, Claus(2006) 'Quasi-static Indentation Measurements: A Tool for Micro-mechanical Investigations of Interfaces in Polymer Materials', International Journal of Polymer Analysis and Characterization, 11: 6, 405 — 418
To link to this Article: DOI: 10.1080/10236660600980250
URL: http://dx.doi.org/10.1080/10236660600980250

International Journal of Polymer Anal. Charact., 11: 405–418, 2006

ISSN: 1023-666X print
DOI: 10.1080/10236660600980250

Quasi-static Indentation Measurements: A Tool for Micro-mechanical Investigations of Interfaces in Polymer Materials

Bernhard Möginger
Fachhochschule Bonn-Rhein-Sieg, University of Applied Sciences, Rheinbach, Germany

Volker Herrmann
Degussa Füllstoffsysteme und Pigmente, Köln, Germany

Claus Unseld
Dunlop GmbH, Hanau, Germany

Abstract: The ongoing use of miniaturization, multi layer structure parts, and hybrid parts requires methods to determine mechanical properties on a micro scale. However, there is a gap in measuring techniques. On one hand there are the classical methods to measure hardness, e.g., Vickers, Rockwell, Universal, and IRHD, having resolutions typically above 100 μm. On the other hand, there are well-developed AFM methods that allow for the determination of mechanical properties in the nanometer range. This article describes an indentation technique that yields data of mechanical properties in the micrometer range between typically 5 and 50 μm. The measuring device and the data evaluation are presented. Results of micro-mechanical mapping are shown for NR-SBR rubber interfaces, a fuel tank, and a part manufactured by two-component injection molding. Finally, the measured micro-mechanical stiffness is compared to the Young's modulus of the corresponding materials.

Received 5 May 2006; accepted 30 August 2006.
Address correspondence to Bernhard Möginger, FH Bonn-Rhein-Sieg, University of Applied Sciences, von Liebig Str. 20, D-53359 Rheinbach, Germany. E-mail: bernhard.moeginger@fh-bonn-rhein-sieg.de

Keywords: Indentation techniques; Interface; Mapping; Micro-mechanical properties; Stiffness

INTRODUCTION

Indentation techniques are the only way to determine local mechanical properties. At the moment there are available classical hardness measurement techniques such as Vickers, Rockwell, Shore A and D, and International Rubber Hardness Degrees (IRHD). The best resolution of these classical hardnesses is achieved by Vickers hardness or its instrumented version, Universal hardness, with a minimum of 40 to 50 μm. However, the intention of these methods is to gain "isotropic" material properties. That means one tries to average over a reasonable number of grains in a metal.

Using an atomic force microscope (AFM) allows determining mechanical properties on a nanometer scale.[1] An AFM is in principle a simple device: a bending bar with a sharp tip at one end having a tip curvature of 10 nm. It can be driven in different modes: the topographic mode, the stiffness mode, and the friction mode.

Each mode yields special structure information of the investigated materials, but the mechanical information is only on a qualitative level. To gain quantitative mechanical information the AFM tip has to be used in an indentation experiment. Then it is possible to measure, for example, stiffnesses of the SAN matrix and the dispersed polybutadiene phase of ABS.[2]

If one is interested in mechanical information on a micrometer scale, e.g., 1 to 100 μm, the AFM technique is capable of delivering it, but because of the nanometer resolution this is time consuming. Furthermore, if there are changes on the micrometer level the nanometer resolution yields a lot of unnecessary information. Therefore, it is desirable to have a method that has micrometer resolution and allows for relatively fast measurements.

THE QSIM INDENTER

The requirements of the QSIM indenter developed and technically realized by Dunlop in Hanau, Germany, are given in Table I.

Using a very slim needle the spatial resolution can be improved by a factor of seven with respect to the Vickers hardness (Figure 1). A table on an arrangement of x-y-z translators is used as a sample holder below the indentation needle. The force measurement and a piezo device allowing additional dynamic oscillations are mounted above the indentation needle (Figure 2).

Table I. Goals and technical requirements of the QSIM indenter

Goal	Requirement
Determination of mechanical properties on a micrometer scale	Slim indenter needle having a tip diameter of approximately 1 μm
Quasi-static mode	PC-controlled indentation procedure via the z translator Very high resolving sensors
Dynamic mode	Superimposing of small sinoidal indentation amplitudes
Mapping mode	x-y translators

THEORY AND EVALUATION

An indentation experiment consists of an indentation step and a retraction step. For plastic and rubber materials, elastic, viscoelastic, viscous, and plastic processes contribute to the indentation curve (Figure 3). In particular, very often adhesion occurs between the indentation tip and the materials surface.

The curvature of the indentation curve depends on hardness and stiffness of the sample, indenter geometry, indentation speed, relaxation behavior of the materials, adhesion between tip and sample, and friction between tip and sample.

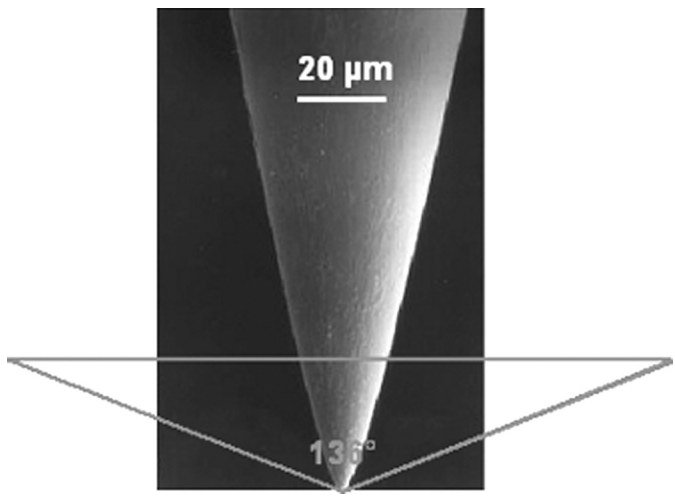

Figure 1. Needle geometry compared to a Vickers pyramid.

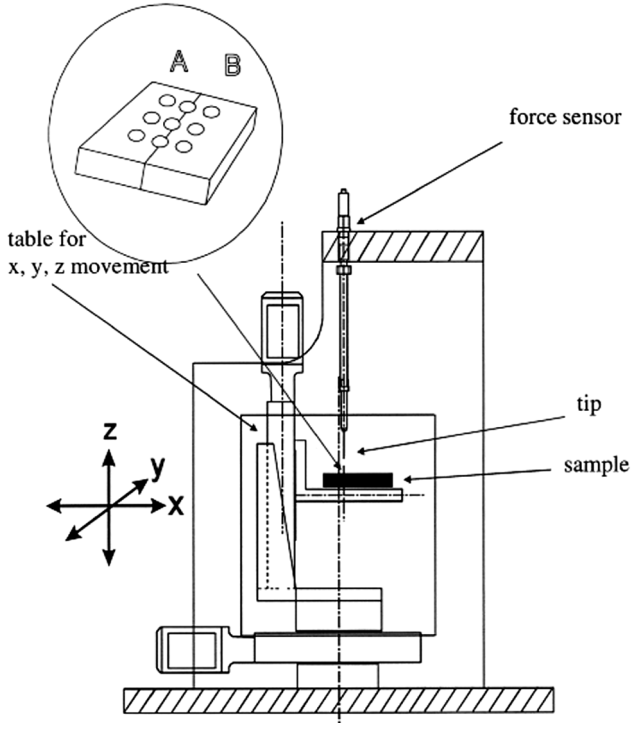

Figure 2. Graphic of the indentation device.

This means that the indentation process becomes very complex if one tries to simulate it in every detail. Figure 4 shows what happens qualitatively for the indentation of a cone indenter. Furthermore, a definition of important quantities such as indentation depth h, contact radius a, cone angle α, and indentation angle β is given. Obviously, there is a very complex stress state consisting of tensile, compressive, and shear stresses around and below the indenter.

To characterize the local mechanical properties it is sufficient to extract some kind of stiffness from the force-indentation curve. Sneddon[3] was one of the first who described the force-indentation curve qualitatively in terms of Young's modulus E, the Poisson ratio μ, indentation angle β, and indentation depth h.

$$F = \frac{2E}{1-\mu^2}\frac{\cot\beta}{\pi}h^2 \tag{1}$$

This description does not satisfy the requirements of plastics and rubbers. Therefore, Maugis and Barquins[4] modified Sneddon's approach

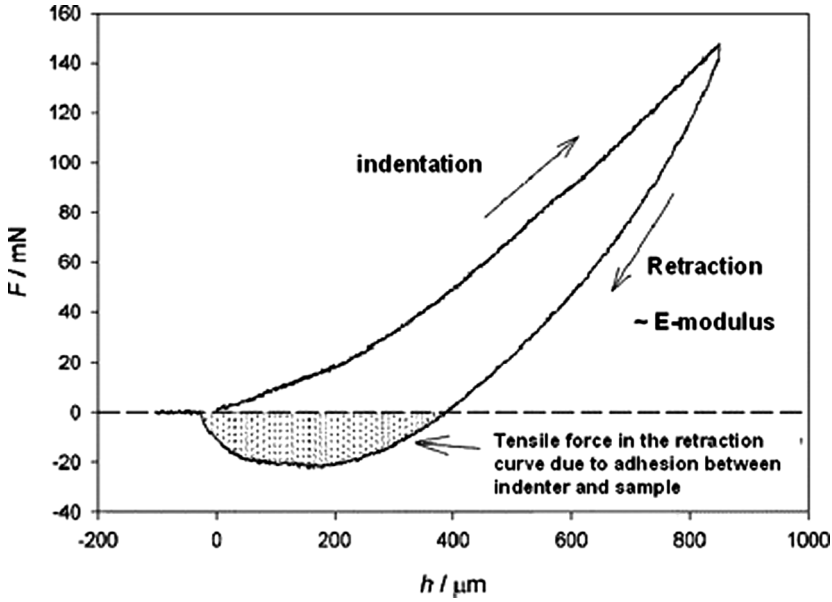

Figure 3. Indentation curve of a rubber.

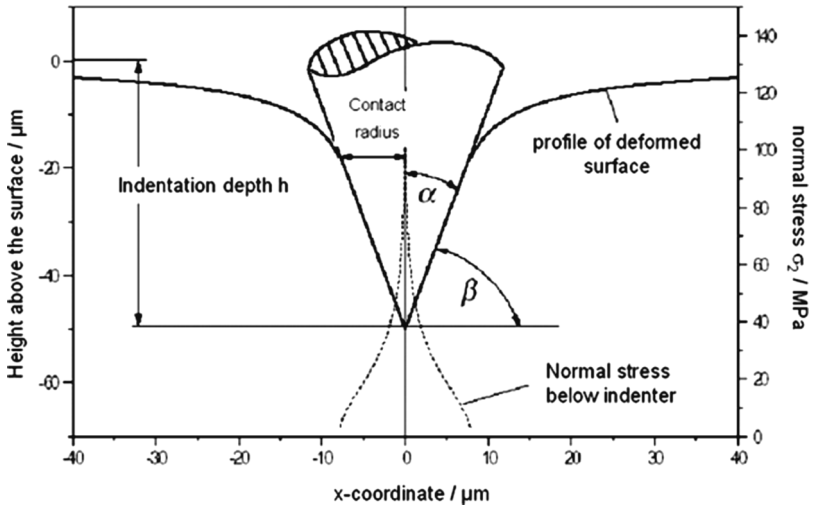

Figure 4. Deformation of the material for an indentation.

with an adhesion term

$$F=\frac{2E}{1-\mu^2}\frac{\cot\beta}{\pi} \times\left[\underbrace{h^2}_{Sneddon}\underbrace{-\frac{2w(1-\mu^2)}{E\tan\beta}\left(2h+\frac{4w(1-\mu^2)}{E\tan\beta}\left(1-\left(1+\frac{Eh\tan\beta}{w(1-\mu^2)}\right)^{\frac{1}{2}}\right)\right)}_{adhesion\ term}\right] \quad (2)$$

containing the thermodynamic adhesion energy w. To evaluate the measured force-indentation curves Equation (2) is used in the form

$$F(h)=k_1h^2+k_2h \quad (3)$$

Differentiation yields

$$\frac{\partial F(h)}{\partial h}=2k_1h+k_2 \quad (4)$$

and the limit for $h\to 0$ yields a term that describes material stiffness for a given indenter geometry:

$$\left.\frac{\partial F(h)}{\partial h}\right|_{h=0}=k_2=S_0 \quad (5)$$

EXPERIMENTAL SECTION

Parameters of the Indentation Experiment

The investigated samples are made of plastic or rubber materials. Those materials show viscoelastic and plastic deformation behavior, and, as a consequence, the measured stiffnesses depend on the parameters chosen for the indentation experiment (Table II).

Table II. Parameters of the indentation experiment

Parameter	Value
Indentation depth	Max. 50 µm
Indentation speed	50 µm/s
Scan distance	$d \geq 4\ a \approx 30$ to 50 µm contact radius a

Table III. Investigated samples

No.	Description of the sample	Processing
1	SBR-NR rubber interfaces	$T_{curing} = 130°/140°/150°/160°C$ $t_{curing} = 200/100/50/\ 30$ min Thickness d = 2 mm and 8 mm Model system for tires
2	PA66GF-rubber interface	Two-component injection molding part made by Bosch for fuel and air intake system
3	Fuel tank made of PE-HD	Coextrusion of seven layers $2 \times PE\text{-}HD_{in}$ – compatibilizer – barrier – compatibilizer – $2 \times PE\text{-}HD_{out}$

Investigated Samples

In order to check the capabilities of the indentation method, samples having internal interfaces were investigated where the mechanical properties of the materials change in different ways. Materials chosen had

- A rubber-rubber interface
- A thermoplastic-rubber interface
- A thermoplastic multi layer structure.

A precise description of the samples is given in Table III.

RESULTS

Rubber-Rubber Interface

A tire is manufactured of several kinds of rubbers, and each rubber has to meet specific requirements in the application. Therefore, it is interesting what mechanical properties occur at the interface of two different kinds of rubber. In order to investigate these interfaces a sample consisting of a styrene-butadiene rubber (SBR) and natural rubber (NR) was cured at different temperatures for different times. The morphology changes significantly with the curing conditions (Figure 5). It is seen that with increasing temperature and thickness the rubbers darken more and more and that there are some changes at the interface.

Determining the materials' stiffnesses according to Equation (5) by a line scan over the interface one finds significant differences of the stiffness

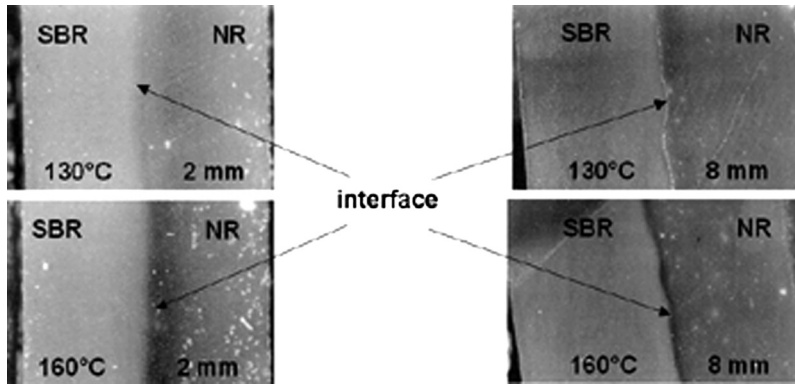

Figure 5. Morphology of the SBR-NR rubber cured at different temperatures and times.

depending on the curing conditions (Figures 6 and 7). At low curing temperatures there is a decrease of the stiffness on the SBR side of the interface, while there is a significant increase of the stiffness on the NR side. With increasing curing temperatures this behavior becomes less pronounced and for a curing temperature of 160°C it has almost vanished.

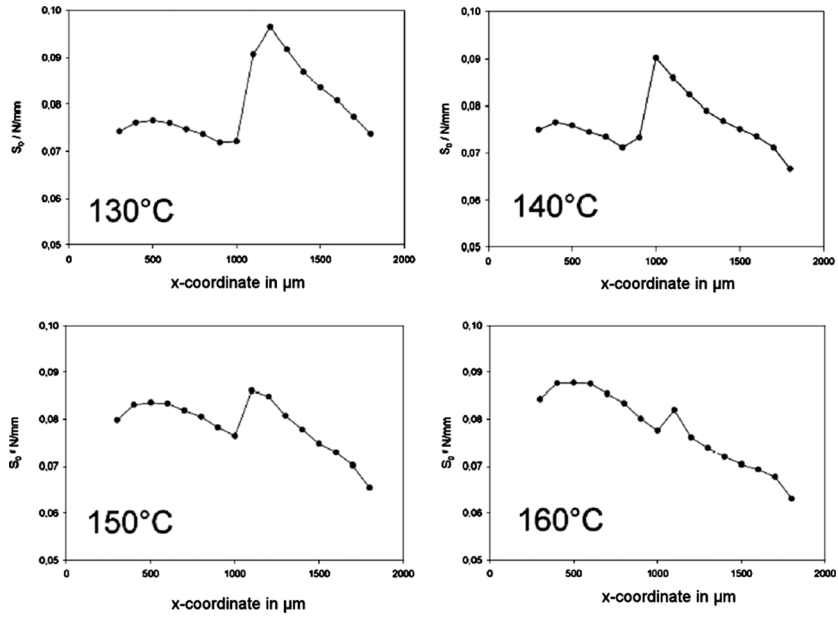

Figure 6. Stiffness line scans over the SBR-NR interface, sample thickness 2 mm.

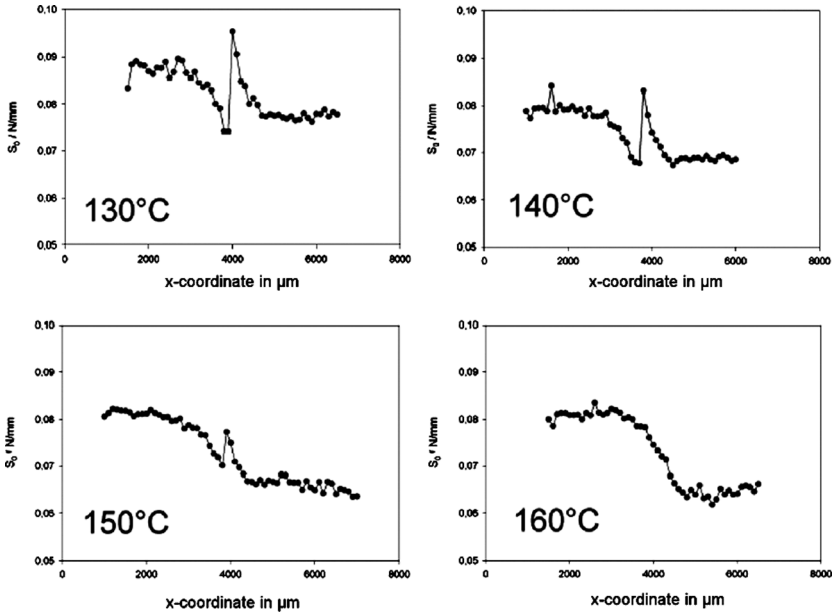

Figure 7. Stiffness line scans over the SBR-NR interface, sample thickness 8 mm.

This phenomenon can be explained only by the fact that the curing agent has a much lower diffusion rate in the SBR rubber than in the NR rubber. As a consequence, at the interface the curing agent diffuses from the SBR phase to the NR phase, leading to a depletion on the SBR side and to an enrichment on the NR side. If the system has enough time for diffusion the stiffness on the NR side increases due to the fact of a significantly higher cross-linking density. The higher the curing temperature the faster the curing process, which leads to the immobilization of the curing agent by chemical reaction, and the less time is available for the diffusion of the curing agent.

Thermoplastic-Rubber Interface

This sample has on one side of the interface a very stiff polyamide 66 reinforced with 30% glass fibers (PA 66 GF), and on the other side there is a very soft silicone rubber (MVQ) of approximately 40 Shore A (Figure 8).

The focus here was to demonstrate that the device is capable of resolving the stiffness jump at the interface quantitatively in a way that

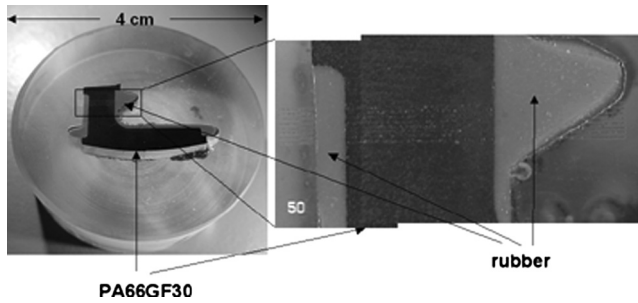

Figure 8. Part with very stiff PA 66 GF and very soft silicone rubber (MVQ).

the measured stiffnesses correspond reasonably to the Young's moduli. Furthermore, in order to prepare the sample for measurement it has to be embedded in epoxy resin. This generates a second interface to both materials and a significantly different stiffness (Table IV). The second question concerns the effect of the glass fibers in the PA 66 on the scatter of the measured stiffnesses.

The line scan starts in the epoxy resin, goes to the MVQ phase, enters the PA 66 GF phase, goes back to the MVQ phase, and ends up again in the epoxy resin (Figure 9). It was found that the stiffness of the epoxy

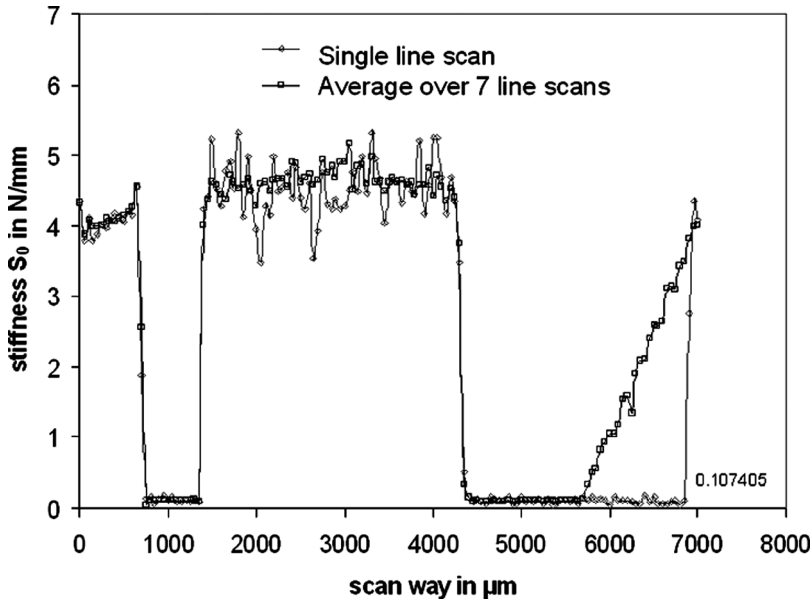

Figure 9. Single line scan (◇) and average over seven line scans (□).

Table IV. Average stiffnesses of the three materials

Material	Stiffness, N/mm	Standard deviation, N/mm
Epoxy resin	4.097	0.115
MVQ rubber	0.110	0.012
PA 66 GF 30	4.670	0.694

resin is increased slightly when approaching the interface of the MVQ rubber phase. Then there occurs a very sharp drop of the stiffness in the MVQ rubber. When entering the PA 66 GF phase the stiffness is increased drastically but shows a broad scatter in the stiffness values. This is, of course, due to the fact that each measuring point on the sample does not hit the fiber underground in the same way. Therefore, one always measures different ratios of PA 66 matrix and glass fiber reinforcement.

Another point has to be kept in mind: in an indentation experiment there is no sensitivity to the fiber orientation. That means effects of fiber orientation on the Young's modulus cannot be determined.

Fuel Tank with Multilayer Structure

The fuel tank consists of seven co-extruded polymer layers (Figure 10).

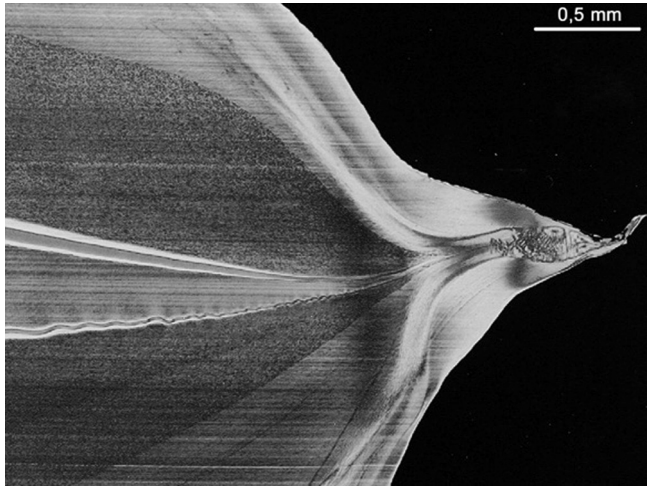

Figure 10. Multi-layer structure of a fuel tank.

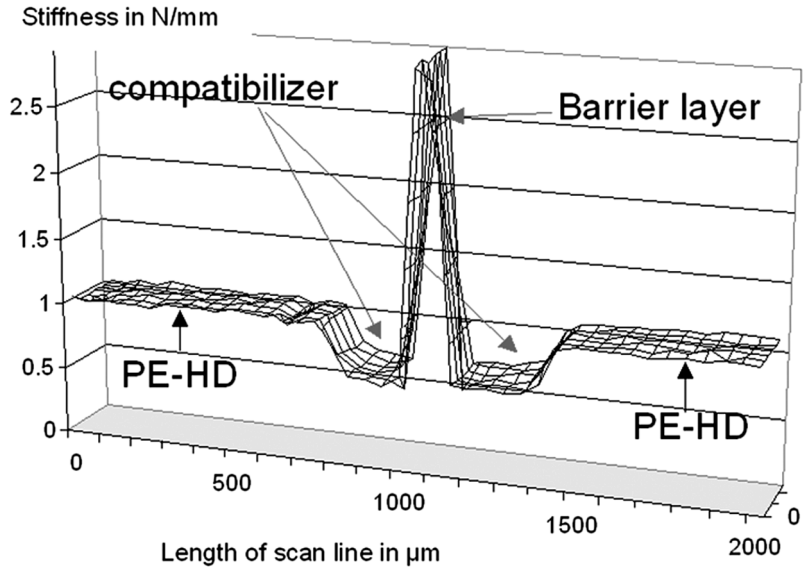

Figure 11. Several line scans over the thickness of the fuel tank.

On each side there are two high-density polyethylene (PE-HD) layers connected to the barrier layer in the center having a thickness of 50 to 100 µm by a layer of compatibilizer. The three materials differ significantly in thickness and modulus (Figure 11).

It can be seen that the stiffness of the barrier layer is significantly higher than that of the PE-HD and the compatibilizer layers. Furthermore, the thickness of the barrier layer is found to be less than 100 µm and the thickness of the compatibilizer layers is slightly higher. Of course, there is no stiffness difference between the several PE-HD layers. The stiffness data are summarized in Table V.

There is a big difference in deformation behavior between thermoplastic and thermosets on one hand and a rubber on the other.

Table V. Stiffness data of the different materials of the fuel tank

Material	Stiffness, N/mm	Standard deviation, N/mm
PE-HD 1	1.038	0.023
Compatibilizer 1	0.665	0.015
Barrier layer	3.017	0.041
Compatibilizer 2	0.694	0.016
PE-HD 2	1.068	0.022

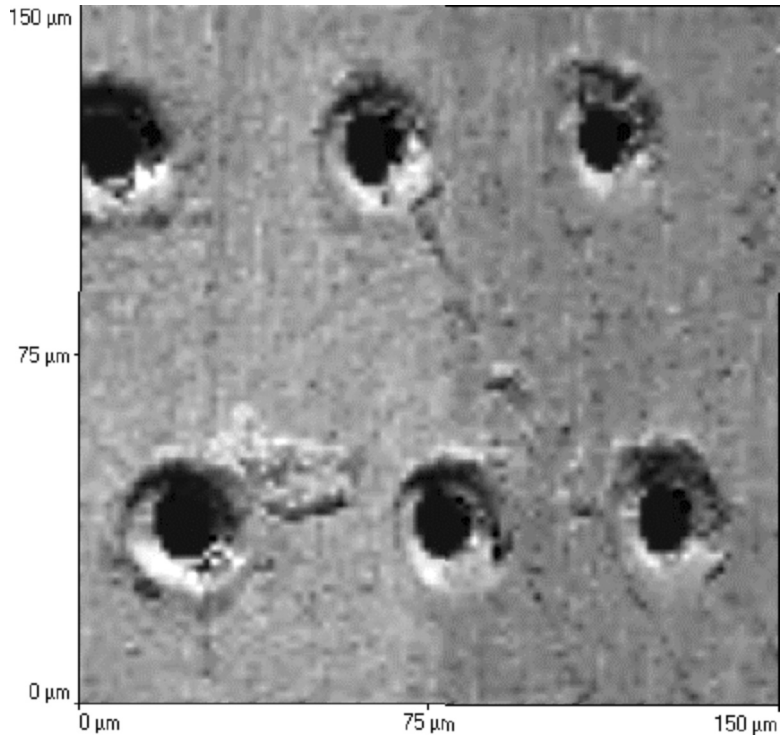

Figure 12. AFM stiffness picture.

The indentation generates in the first case a remarkable amount of plastic deformation (Figure 12), while a rubber almost fully recovers. Figure 8 shows no indentation points in the rubber phases.

This remarkable amount of plastic deformation indicates that for thermoplastics and thermosets the indentation depth can be significantly

Table VI. Indentation stiffness and Young's modulus of the materials

Material	Stiffness, N/mm	Young's modulus, MPa
Epoxy resin	3.7 to 4.2	3200 to 4000
PA 66 GF 30	4.0 to 5.4	7200 to 10000
Barrier layer	3.0 to 3.1	≈2400
PE-HD	1.0 to 1.1	800 to 1200
Compatibilizer	0.7	≈500
MVQ rubber	0.1	1 to 2
SBR rubber	0.072 to 0.084	≈1
NR rubber	0.068 to 0.080	≈1

reduced. This would decrease the plastic deformation and enhance the spatial resolution. For rubbers this indentation depth is necessary to achieve measurable indentation forces.

CONCLUSION

Indentation techniques using very slim needle-like indenters allow mapping and measuring stiffnesses of materials on a micrometer scale. As the indentation depth is 50 μm, the typical contact radius is around 10 μm. But for stiffer materials such as thermoplastics or thermosets the indentation depth can be reduced to less than half, leading to a lateral resolution of less than 20 μm.

The indentation stiffnesses correlate quantitatively with the Young's moduli of the materials, but have different orders of magnitude and different dimensions (Table VI). In particular, the correlation becomes difficult if short fiber reinforced materials are tested, as one is dealing with a compressive deformation state rather than with a tensile one.

REFERENCES

[1] Bhushan, B. and O. Marti. (2004). Scanning probe microscopy—Principle of operation, instrumentation, and probes. In *Springer Handbook of Nanotechnology*, ed. B. Bhushan. Heidelberg: Springer-Verlag, pp. 325–369.
[2] Möginger, B. et al. (2001). Determination of mechanical stiffness in microphases of ABS model materials using AFM indentation. *Series Adv. Exp. Mech.* **6**, 95–97.
[3] Sneddon, I. N. (1948). Boussinesq's problem for a rigid cone. *Proc. Camb. Philos. Soc.* **44**, 492–507.
[4] Maugis, D. and M. Barquins. (1981). Adhesive contact of a conical punch on an elastic half-space. *J. Phys. Lett.* **42**, 95–97.